Icarus 204 (2009) 262–270

Contents lists available at ScienceDirect

Icarus

journal homepage: www.elsevier.com/locate/icarus

Grooves on small saturnian satellites and other objects: Characteristics and significance

Sarah J. Morrison *, Peter C. Thomas, Matthew S. Tiscareno, Joseph A. Burns, Joseph Veverka

Cornell University, Center for Radiophysics and Space Research, Space Sciences Building, Ithaca, NY 14853, USA

ARTICLE INFO

Article history:
Received 23 April 2009
Revised 1 June 2009
Accepted 3 June 2009
Available online 13 June 2009

Keywords:
Saturn
Satellites, Surfaces
Satellites, Shapes
Satellites, Dynamics

ABSTRACT

High-resolution images from the Cassini Imaging Science Subsystem (ISS) show parallel sets of grooves on Epimetheus and Pandora. Grooves have previously been observed on other satellites and asteroids, including Phobos, Gaspra, Ida, Eros, and minor occurrences on Phoebe. Sets of parallel grooves are so far observed only on satellites known or likely to be subject to significant tidal stresses, such as forced librations. Grooves on asteroids and on satellites not subject to significant forced librations occur in more globally disorganized patterns that may reflect impacts, varying internal structures, or even thermal stresses. The patterns and individual morphologies of grooves on the tidally-affected satellites suggest fracturing in weak materials due to tidal stresses and forced librations.

1. Introduction

The Cassini spacecraft exploration of the saturnian system of satellites examines diverse characteristics ranging from the satellites' dynamical properties to surface geology. Surface properties and geological histories of small bodies are particularly challenging to study due to limited opportunities to get spatially well-resolved data. The length of the Cassini mission, however, has now allowed enough views of some of the small saturnian satellites to characterize the geology and make useful comparisons among them and to other systems. One of the features observed on some small saturnian satellites, sets of linear surface depressions referred to as grooves, are particularly significant because of their occasional, but not universal occurrence on other bodies, and the long-standing debates on their origins.

Phobos was the first small Solar System body to be imaged in high resolution. The Viking Orbiter images revealed that the surface has groups of long, parallel depressions, termed grooves (Veverka and Duxbury, 1977). These unexpected features signaled that processes on small bodies might be more complex than simple impact gardening. Subsequent missions have found grooves on the small asteroids Gaspra, Ida, and Eros (Veverka et al., 1994; Sullivan et al., 1996; Prockter et al., 2002), and minor ones on Saturn's satellite Phoebe (Porco et al., 2005). Grooves are notably absent from Deimos and from asteroid Mathilde (Veverka et al., 1997). Asteroid Steins (Keller et al., 2008) shows a chain of large craters, but was not imaged well enough to detect grooves of form or scale similar to those observed on other objects. Galileo and Voyager data on small satellites were not of sufficient resolution to detect or rule out grooves on the small satellites elsewhere in the outer Solar System. There are, of course, many forms of grooves associated with internally-driven tectonics on larger satellites such as Europa, Ganymede, Enceladus, and Miranda, and major fracture systems on others, such as Dione and Tethys, and Mimas (Pappalardo, 2006). Here we limit our study to objects small enough to lack internally-driven tectonics and significant effects of viscous relaxation (<∼200 km radius).

2. Data and methods

The Cassini Imaging Science Subsystem (ISS) is described in Porco et al. (2004), and has two 1024 × 1024 pixel detectors, one with 0.35° FOV, the other 3.5° FOV. The Narrow Angle Camera (NAC) provides images of 6 km/pixel at 10^6 km range. The Cassini orbital tour is tied to repeated flybys of Titan at 20.3 Saturn radii, with changing periods, eccentricities, and inclinations. Thus, images of the small satellites, most of which orbit close to Saturn, have a non-systematic distribution over the satellites' surfaces. The best pixel scales on the small satellites obtained as of December 2008 are shown in Table 1. Available image properties for comparison objects are described below as appropriate.

Mapping of features has been done interactively, marking positions and sizes on shape models derived from stereogrammetry and limb matching. Mapping first required solution of complications such as forced librations of Epimetheus and changing orbital periods after the orbit swap of Janus and Epimetheus (Tiscareno et al., 2009) in order to have the accurate body-centered geometry

* Corresponding author.
E-mail address: sjm276@cornell.edu (S.J. Morrison).

0019-1035/$ - see front matter © 2009 Elsevier Inc. All rights reserved.
doi:10.1016/j.icarus.2009.06.003

Table 1
Observations of small objects.

Object	$R_{m,\ km}$	ρ (kg m^{-3})	g (cm s^{-2})	Best res (m)	Res/radius	Grooves (blank = not yet determined)
Pan	14.2 ± 1.3	410 ± 150	0.01–0.18	1260	0.089	
Daphnis	3.9 ± 0.8	310 ± 200	0.01–0.04	1900	0.49	
Atlas	15.1 ± 1.4	460 ± 160	0.02–0.20	249	0.016	
Prometheus	43.1 ± 2.6	480 ± 90	0.13–0.58	2610	0.06	
Pandora	40.7 ± 1.5	490 ± 60	0.26–0.60	312	**0.008**	**Yes**
Epimetheus	58.1 ± 1.8	640 ± 60	0.65–1.1	226	**0.004**	**Yes**
Janus	89.5 ± 1.4	630 ± 30	1.1–1.7	178	**0.002**	**No**
Methone	1.6 ± 0.6			1300	0.081	
Pallene	2.5 ± 0.6			456	0.21	
Telesto	12.3 ± 0.4			84	**0.007**	**Yes**
Calypso	10.6 ± 0.7			600	0.06	
Polydeuces	1.3 ± 0.4			384	0.30	
Helene	17.6 ± 0.4			230	**0.013**	**No**
Hyperion	135 ± 4	544 ± 50	1.7–2.1	20	**0.00015**	**No**
Phoebe	106.5 ± 0.7	1629 ± 50	3.8–5.0	14	**0.00013**	**Yes**
Phobos	11.1 ± 0.1	1867 ± 62	0.35–0.66	5	**0.0005**	**Yes**
Deimos	6.2 ± 0.2	1540 ± 220	0.26–0.34	5	**0.0008**	**No**
Gaspra	6.1 ± 0.4			164	**0.026**	**Yes**
Ida	15.7 ± 0.6	2600 ± 500	0.31–1.02	31	**0.0020**	**Yes**
Eros	8.3 ± 0.05	2640 ± 20	0.24–0.56	4	**0.0005**	**Yes**
Mathilde	26.5 ± 1.3	1300 ± 200	~0.9	230	**0.0087**	**No**
Itokawa	0.16 ± 0.002	1900 ± 130	~0.01	<1	**0.006**	**No**

Saturnian satellite dimensions are from Thomas (2009) which include updates from values in Porco et al. (2007); masses used are from Porco et al. (2007) and Jacobson et al. (2008). Phobos and Deimos sizes from Thomas (1993); masses from Konopliv et al. (2006). Gaspra data from Thomas et al. (1994); Ida data from Thomas et al. (1996); Eros from Thomas et al. (2002); Mathilde from Thomas et al. (1999); Itokawa from Fujiwara et al. (2006).
Bold values for resolution/radius are those equal or better than Gaspra observations, the lowest relative resolution for which grooves are found.
The two possible grooves on Janus are not counted toward definite groove observation.

of the spacecraft necessary for consistent shape model fitting. We have also remapped grooves on Phobos, using the Viking Orbiter data set as well as some images from HRSC (Neukum et al., 2000) to fill out the geometry of those grooves.

3. Grooves on small objects

Cassini images show unambiguous grooves only on Epimetheus, Pandora, and Phoebe (Figs. 1 and 2; Table 1; grooves on Epimetheus and Pandora are initially discussed in Morrison et al., 2008). Table 1 summarizes a variety of properties of small satellites and asteroids, the resolution of the imaging data, and whether grooves are apparent. Gaspra provides the most marginal instance of groove detection. Other objects with relative image resolution better than that on Gaspra that do not show grooves are Hyperion, Telesto, Helene, Deimos, and comet nuclei. Images of Amalthea (mean radius 88 km) at a few km/pixel do not show grooves. The uranian small satellites were imaged at low resolutions (4.5 km pixel or worse) and their shapes barely detected. Neptune's Proteus (mean radius of 208 km) had suggestions of linear markings at 1.3 km/pixel, but the very low signal-to-noise of the best image renders almost any surface interpretation suspect (Croft, 1992).

3.1. Characteristics of grooves on saturnian satellites

Grooves on Epimetheus are commonly 5–20 km in length (Table 3). Many have slightly sinuous boundaries with varying widths; a few have straight, nearly parallel walls with well-defined breaks in slope between walls and floors. These latter forms are characteristic of graben topography (Fig. 3). These provide strong evidence of failure with tension (or minimal compression) perpendicular to the length of the groove, or along the satellite's long axis direction. The graben form primarily indicates that vertical stress is the greatest compressive one (Van der Pluijm and Marshak, 2004). Widths of Epimetheus' grooves average about a km (Table 2), with a modest range of values. As with grooves on other objects, the occasional impression of raised rims cannot be taken as evidence of constructional topography due to interference from nearby grooves, albedo features, and somewhat limited resolution. The grooves on Epimetheus primarily fall into a pattern that runs parallel to the intermediate axis of the satellite (Figs. 1 and 4) with some tracing directions about 60° from the majority set. The latter group appears more beaded and pitted, and more sinuous in shape. Because of the minimal curvature where these grooves occur (what is most likely a very degraded, ~90 km crater), and because the grooves cover less than 20° of arc, fitting planes to the surface traces of these forms is not a productive exercise.

The context for the Epimetheus grooves is shown in Fig. 1b. Epimetheus is a heavily cratered object, with crater populations close to empirical saturation (Richardson and Thomas, 2007). Craters show a range of degradation states, although a large proportion retain distinct raised rims. Loose material with a relatively smooth surface has collected in many craters and other low points (Fig. 1a). There appear to be two types of filling material, perhaps two generations of debris, likely ejecta reaccreted to the satellite. The large crater at the lower left of Fig. 1 illustrates the different fill materials, though the difference can be seen in a few other craters. The smooth appearance of substantial parts of the object may be simply due to covering by this loose material. Many saturnian satellites have a relative deficiency of 1–10 km craters (Richardson and Thomas, 2007) and this relative deficiency may abet the smooth appearance of this object.

Pandora's grooves reach nearly 30 km in length (Fig. 2), though most are substantially shorter. Widths are nearly the same as those on Epimetheus. The Pandora grooves largely fall into a pattern of parallel members that, from a north polar view, trend ~30° from the intermediate axis direction (Fig. 4). These grooves are slightly less well imaged than the Epimetheus ones (Table 1), so details of their morphology are more difficult to decipher. As far as is visible, the grooves in Fig. 2 have little variation in widths along their lengths. A few of the craters on Pandora also show filling by smoother materials, which is additional indication of loose, regolith material and probably of ejecta reaccretion.

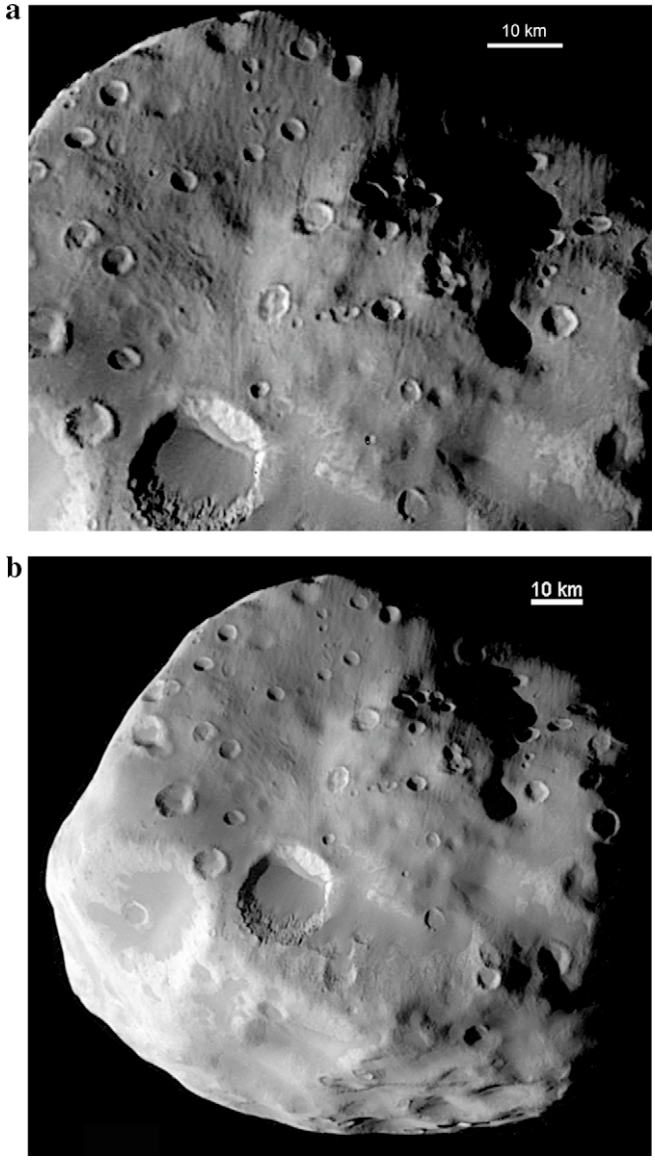

Fig. 1. Grooves on Epimetheus. (a) Filtered, stretched portion of image N157536313. (b) Full disk context of (a).

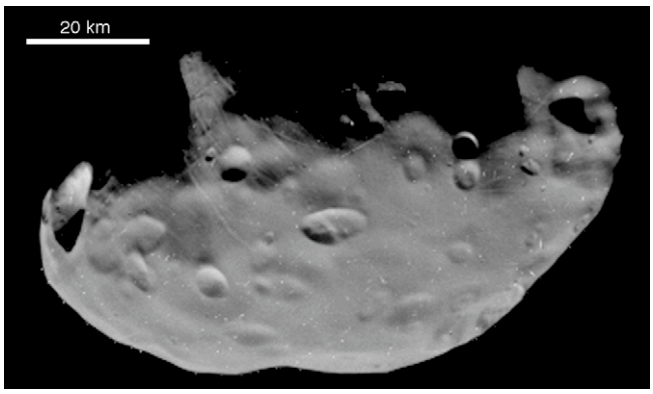

Fig. 2. Grooves on Pandora. Cassini image N1504613650. Grooves are most prominent in upper left quadrant. There are numerous cosmic ray tracks (short white lines in random directions) visible. Inspection of multiple images insured the mapped grooves were not misinterpretations of cosmic ray signatures.

The grooves on Phoebe are seen only in some of the highest resolution images (Porco et al., 2005), and there are no global or substantial regional groups such as on Pandora or Epimetheus. Widths relative to object radius are much smaller (Table 2) than for Epimetheus and Pandora, and the lengths are smaller and instances more discontinuous than for the other objects. These grooves are mostly very shallow forms; even the widest appear to have slopes well under 15°, implying total depths under 15 m. Some have fairly straight boundaries, but many have significant variations in widths and even beaded appearances (Porco et al., 2005, Fig. 3f).

Janus displays two possible examples of single grooves in the highest resolution images (N1593509761; 178 m/pixel), one about 6 km long, the other nearly 10 km long, both ~0.7 km wide. These are separate features, not part of a cluster. Only a small portion of the satellite has been viewed at such good resolutions. Other polar views at 950 m/pixel (effectively almost three times the relative resolution of Gaspra images with grooves), with good illumination over significant areas, show no grooves.

3.2. Small saturnian satellites without grooves

Imaging of Telesto, Helene, and Hyperion is more than adequate to show grooves similar to those on Epimetheus and Pandora. Although images of Helene do include some with high resolution, they only cover a small area (viewed at high solar phase angle). Hyperion's rough, sponge-like surface does not display grooves. Excellent imaging of Telesto, as good as 84 m/pixel, shows a heavy covering of debris partially filling craters and undergoing downslope transport. There are no obvious linear features, pit rows, or the like on Telesto.

3.3. Grooves on Phobos

Phobos shows the greatest concentration and relative area coverage of grooves on any object imaged to date. The great majority of Phobos' grooves belong to a few sets that define planes approximately parallel to the intermediate axis of the object (Thomas et al., 1979). These grooves occur as both single forms and as side-by-side arrangements with very consistent widths for distances of kilometers. Some morphologically continuous grooves switch from one planar set to another. Most Phobos grooves have muted to obvious pitted appearances. Raised rims may exist on some grooves, but in most instances their presence is hard to establish because of adjacent groove depressions and common, relatively brighter albedo features. A few show graben-like morphology (Fig. 3). The deepest, widest, and greatest concentration of grooves is near the large crater Stickney, but some grooves postdate the crater and the pattern is not radial to the crater. Some of these very wide grooves taper into lengthy, but much narrower depressions.

3.4. Grooves on asteroids

Asteroids Eros and Itokawa are, by far, the best investigated. Eros' grooves occur in many locations and patterns (Thomas et al., 2002; Prockter et al., 2002; Dombard and Freed, 2002; Buczkowski et al., 2008). Eros grooves are generally less than 2 km long; widths are typically 75–100 m with a maximum of about 200 m (Prockter et al., 2002). Depths are probably well under 20 m. Outlines are variable with a typically beaded appearance, though they rarely show clear sets of pits. The global patterns are shown in Fig. 4.

Gaspra's grooves, marginally resolved, are common on the well-imaged portion of the asteroid (Veverka et al., 1994; Carr et al., 1994). Most grooves are less than 1.5 km in length; widths are

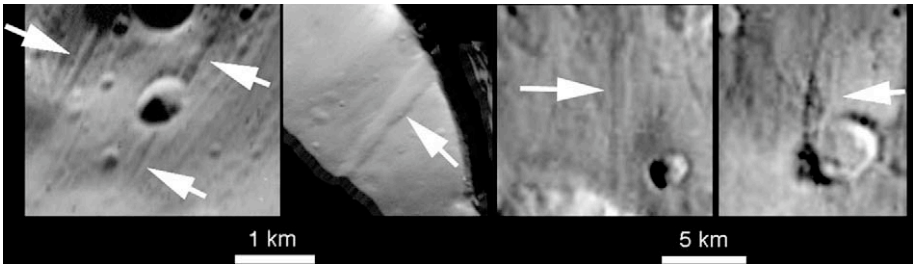

Fig. 3. Portions of grooves on Phobos and Epimetheus showing graben-like morphology (arrows). Phobos left two panels; Epimetheus right panels.

Table 2
Groove widths.

Object	Mean width (km ± s.d.)	Pixel scale (m)	Number measured	Width/ radius
Pandora	1.04 ± 0.23	313	30	0.026
Epimetheus	1.06 ± 0.24	226	59	0.018
Phoebe	0.24 ± 0.13	20	383	0.0023
Phobos	0.13 ± 0.055	8	307	0.012
Eros	~0.09	4	[a]	0.011
Gaspra	~200 m	164	[b]	0.032
Ida	~100 m	31	[c]	0.016

[a] Prockter et al. (2002).
[b] Veverka et al. (1994).
[c] Sullivan et al. (1996) and Asphaug et al. (1996).

barely resolved at 100–200 m (Tables 2 and 3). They have a straight-walled to pitted appearance. Although some are crudely parallel, and might reflect something of a global fabric (Veverka et al., 1994), their lengths are very short compared to the size of Gaspra and the spread of orientations (Veverka et al., 1994, Fig. 3c) so great, they present a haphazard pattern compared to those on Phobos and Epimetheus.

Itokawa has been completely imaged, with some areas covered by images <0.1 m/pixel (Fujiwara et al., 2006). This small (160-m mean radius) object is an obvious collection of rubble, with strong particle size sorting forming some smoother areas in gravitational lows (Saito et al., 2006). No forms similar to grooves are present.

Mathilde, imaged at 230 m/pixel, shows no grooves on the visible portion (Veverka et al., 1997). The only possible structural feature is a band that may be an exposed layer.

3.5. Grooves and comet nuclei

The two comet nuclei imaged at high resolution, Wild-2 and Tempel-1, show no evidence of grooves among the plethora of other interesting forms (A'Hearn et al., 2005; Brownlee et al., 2004). Two different types of layering are visible on Tempel-1 (Thomas et al., 2007), and steep slopes, overhangs, and round depressions with flat floors characterize Wild-2.

4. Groove origins

Since the discovery of grooves on Phobos (Veverka and Duxbury, 1977), their formation mechanisms have been extensively debated. Proposed mechanisms generally fall into three categories: (1) reaction of the regolith to fracturing, with various causes of the fracturing (Thomas et al., 1979; Soter and Harris, 1977; Weidenschilling, 1979), (2) tracks of rolling or reimpacting ejecta on the satellite (Head and Cintala, 1979; Wilson and Head, 2005), and (3) ejecta from Mars (Murray et al., 1994, 2006). We briefly review some of the characteristics of these mechanisms and why the fracturing mechanisms are so far the best hypotheses for the vast majority of grooves. The systematics of groove characteristics on different bodies are then used to infer more details of possible origins.

4.1. Phobos groove origins

We do not subscribe to the rolling ejecta hypothesis because Phobos' grooves follow paths at a wide range of angles to local slopes, and because of the lack of remaining large ejecta blocks, some of which would need to be well over 100 m in diameter. The transitions from some very large and deep grooves to much narrower and shallow ones, with consistent widths over a variety of topography seem inconsistent with rolling debris trails. The grooves also bear little resemblance to ejecta-formed gouges on Eros (Robinson et al., 2002; Durda, 2009). Comparison of groove patterns with ejecta emplacement models were presented in Thomas (1998) and showed most groove patterns to be inconsistent with possible secondary ejecta patterns. The Mars ejecta hypothesis (Murray et al., 2006), which would entail covering significant parts of Phobos with close-packed impacts, would require that Mars be covered many times over by secondary impacts of >50 m objects, and would also require a significant fraction of the Phobos regolith to be Mars-derived materials. In addition to needing vastly greater amounts of Mars ejecta to reside on Phobos than thought possible (Gladman, 2007), the mechanism for providing collimated, closely aligned ejecta streams thousands of kilometers from an impact site after being launched at a large fraction of Mars' escape velocity is implausible.

The morphology and patterns of grooves on Phobos do, however, match expectations of fracturing, with some regolith response. The pattern is strongly suggestive of extension along the long axis, as expected from tidal theory (Soter and Harris, 1977; Weidenschilling, 1979). The morphology is consistent with regolith drainage into cracks, partial compaction, or graben modification (Thomas et al., 1979; Horstman and Melosh, 1989). The switching of grooves between planar sets is an expected characteristic of fracturing. The planar pattern defined by most Phobos grooves is very well measured (Thomas et al., 1979), and certainly indicates that the body's principal shape axes play a key role in determining the occurrence of the grooves. The relative ages of different sets is not always clear, but the set perpendicular to the long axis appears cut by most other grooves and is thus the oldest (Thomas et al., 1979). Those parallel to the equator are intermediate in age, and the youngest of the three most prominent sets are those oriented between the long and short axes of Phobos.

Not all of Phobos' grooves have the same morphology or follow the main patterns, and this leaves open the possibility of multiple origins. Fracturing from Stickney may have expanded fractures already in place, exploiting a tidal pattern but making them most obvious near the large impact. Three of the very wide, hummocky grooves (Thomas et al., 1979) are sufficiently distinct that they may require different explanations, perhaps including secondary effects from large impacts. These are the only ones that can be

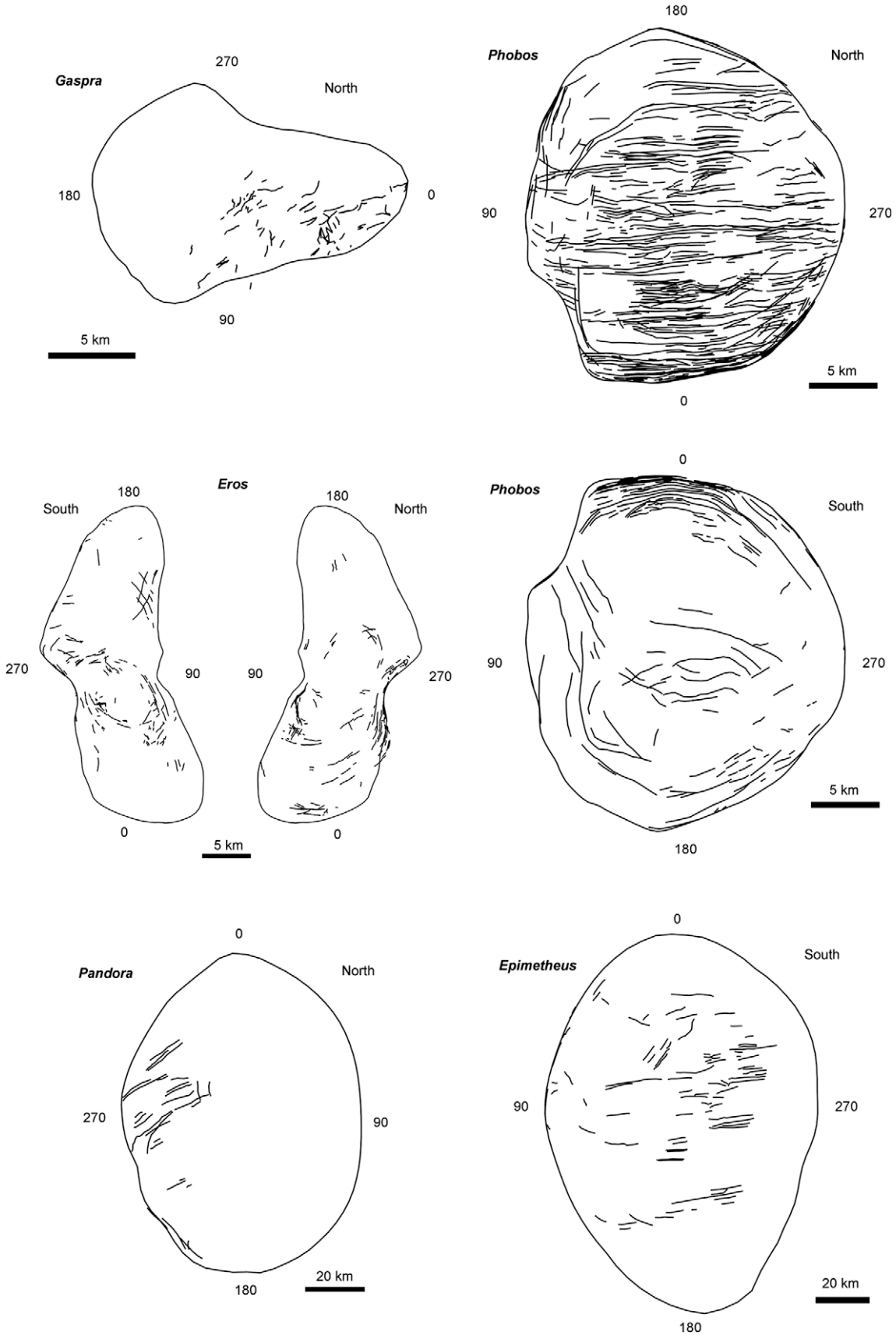

Fig. 4. Polar projected views of grooves on satellites and asteroids. Projections are with equatorial profiles; grooves may project beyond the equator in some places.

approximated by predicted trains of secondary impacts from Stickney (Thomas, 1998). The vast majority of Phobos' grooves, however, do not fit this category, and cannot be reconciled with any ejecta scheme.

Table 3
Groove characteristics.

Object	Max/mean lengths (in km)	Degrees of arc for mean length	Morphology	Patterns	Relative ages
Pandora	20/11	16	Straight (beaded)	One parallel set	?
Epimetheus	25/10	11	Beaded; straight	Most parallel to intermediate axis; one additional set	?
Phoebe	7/3	1.6	Beaded; tapering	Various	?
Phobos	19/6	31	Beaded, pitted, straight	Four primary parallel sets	Clear age superpostions
Eros	8/2	14	Beaded, pitted	Various	?
Gaspra	2.5/1.5	14	Beaded to straight	Crossing; one nearly parallel set	?
Ida	3/1.5	3	Beaded to straight	Parallel to radiating	?

Tidal stresses (Aggarwal and Oberbeck, 1974) were invoked by Soter and Harris (1977) to explain the orientation of Phobos' grooves that defined planes normal to the satellite's long axis. Their specific application was the increasing tensile component as Phobos' orbit evolved inward (Burns, 1978, 1986). Weidenschilling (1979) proposed an alternative theory in which stresses caused by non-synchronous rotation induced by the large Stickney impact within a strong tidal field could produce fracturing consistent with the observed patterns. Weidenschilling (1979) specifically predicted that if tidal stresses are necessary for "regular systems of grooves", then such objects as Deimos that orbit far from the primary would not be expected to have such features.

4.2. Groove origins on asteroids

Grooves on Gaspra and Eros (Fig. 4) do not have the well-organized global pattern found on Phobos. The Eros grooves have been attributed to local impact effects (Prockter et al., 2002; Buczkowski et al., 2008), with some possible instances of influence by preexisting internal structures. Fractures caused by global thermal changes with an evolving orbit also have been invoked to explain the patterns of some grooves on Eros (Dombard and Freed, 2002). The largest relatively fresh crater on Eros, over 7 km in diameter, appears to have generated still-visible numbers of blocks a few m to 150 m across. There is at least one instance of a block being clearly associated with a short regolith gouge (Robinson et al., 2002), but the lack of boulders associated with any others of the hundreds of grooves would seem to eliminate that mechanism as a plausible general groove-forming process. It is likely that Eros' grooves are primarily related to fractures, but there may be multiple sources of stress as well as the influence of preexisting structures. Due to marginal resolution, we cannot describe the Gaspra groove origins in detail. They are not associated with individual impact craters, and while having two different sets of crudely parallel members, they do not cover large arcs on the surface. A few do show the combination of directions from the two sets in single grooves, again a strong sign of fracture influence.

Asteroid Ida has grooves clustered in one group, almost a parallel set, but with a slightly flared pattern (Sullivan et al., 1996). Asphaug et al. (1996) used impact crater modeling to infer that these grooves most likely reflect fractures from a 12-km crater on the opposite side of Ida. There is, however, no global set of grooves on Ida, and the area covered by these visible grooves is only a few percent of the well-imaged part of the asteroid (itself slightly less than 50% of the whole asteroid surface).

4.3. Groove origins on the saturnian satellites

The pattern of grooves on Epimetheus is consistent with tensile stresses along the length of the object, most easily associated with tidal effects. The graben form primarily indicates that vertical stress is the greatest compressive one. Here this would be, at a minimum, on the order of ρgh, where ρ is probably $\sim$0.6 g cm^{-3}; g is $\sim$1 cm s^{-2}, and $h \sim 20$ m (2000 cm) so $\rho gh \sim 1200$ dyne cm^{-2} or 120 Pa. The depths of the steeply dipping faults bounding the graben are probably slightly less than total graben width, or here $\sim$1 km depth, for a normal stress of $\sim$6000 Pa.

4.4. General groove origins

We address which objects have well-organized grooves and which do not to limit possible formation mechanisms. Among satellites, the first difference in occurrence correlates with orbital distance from the primary. Phobos, Pandora, and Epimetheus orbit at 2.76, 2.35 and 2.51 primary radii, whereas those synchronously rotating and clearly lacking grooves, Deimos and Telesto, orbit at 6.91 and 4.88 planetary radii. Hyperion and Phoebe, which we consider not to have a similar set of grooves, are far from Saturn and do not spin synchronously with their orbital periods and thus are not subject to repetitive tidal stresses with consistent body-fixed orientations; tidal stresses at great distances are also negligible. Janus, co-orbital with Epimetheus, orbits close to Saturn and does not have a global groove pattern similar to that of Epimetheus. In reference to the discussion below, we note that Janus has no measured physical libration, and an optical libration of only 0.8° (Tiscareno et al., 2009).

While some grooves show sharply bounded margins, most have concave-up profiles, frequently beaded outlines, and a generally smooth transition to their surroundings. These morphological differences may simply reflect different ages, and/or different material properties. All groove shapes seem consistent with formation in weak or loose materials affected by deeper mechanical processes. Drainage of the regolith has been suggested as the primary method of formation in fracture-related scenarios. Thomas et al. (1979), and others, particularly Horstman and Melosh (1989), dealt with some ramifications of removing regolith. The latter authors, in particular, concluded from laboratory simulations that pit spacing could be used to infer regolith depth. Their study suggested depths of loose regolith material on Phobos in excess of 200 m.

Table 2 shows that with the exception of Phoebe's, grooves on these objects have widths $\sim$1–3% of the object's mean radius. This characteristic might mean that regolith depths on these objects have crudely similar relations to object size. A regolith depth/object size relation can follow from ejecta accumulation and gardening between large impacts since the deeper the regolith, the less new regolith is generated during further impacts (Housen and Wilkening, 1982). Porco et al. (2007) proposed that ring-related satellites such as Pandora have shapes indicative of accretion of a thick blanket of low-density material over a denser core (not applicable to Epimetheus). The widths of the Pandora grooves suggest regolith depths, or depths to denser regolith, of less than several hundreds of meters. This interpretation as well as Pandora's heavily cratered surface (Fig. 2) indicate that the grooves are probably not a discriminating probe of any such accretional, deep features on this object.

Both Telesto and Deimos have deep regolith coverings that might be postulated to hide grooves. However, Deimos' covering is of variable depth, and there is excellent imaging (<2 m/pixel) in the polar area where grooves are so prominent on Phobos

(Thomas, 1998). Additionally, regolith is part of the fracture origin hypothesis, and grooves seem to indicate deep regolith on parts of Phobos. The considerable amount of smooth crater fill on Telesto exhibits widespread downslope transport, and as with Deimos, should vary in thickness in an area of similar grooves. Telesto's imaging (Table 1) is also excellent for finding even hints of such forms. Thus, we conclude these two objects have not formed grooves similar to those on Phobos, Epimetheus, and Pandora, and the distinction may be due to tidal stresses.

5. Tidal stresses and grooves

As a first step to estimate tidal stresses, we consider the tidal distortion of a homogeneous fluid satellite in an un-inclined circular orbit. Such bodies are shaped by two potential fields: *centrifugal effects* ($\sim\omega^2 \cdot r^2$, where ω is the spin rate and r is the distance from the spin axis) that lead to an oblate, rotationally flattened body whose shortest dimension lies along the spin axis; and *tidal effects* ($\sim GMr^2/R^3$, where G is Newton's gravitational constant, M is the planet's mass and R is the satellite's orbital radius) that produce a prolate shape with the long axis pointing toward the planet. When both fields are present, fluid satellites would become triaxial ellipsoids (of semi-axes $a > b > c$) with the longest axis (a) pointing toward the planet and the shortest (c) normal to the orbit plane. The relative distortions from a sphere are +7:−2:−5 (Squyres and Croft, 1986, p. 320; Murray and Dermott, 1999, p. 156). Centrifugal and tidal effects can be shown to be comparable by expressing the satellite's mean orbital angular velocity $n = (GM/R^3)^{1/2}$ from Kepler's third law, or by simply balancing the central gravity against the centripetal acceleration; note that $n = \omega$ because the body is assumed to be rotating synchronously. Hence maximum stresses are $\sim\rho\omega^2 r^2$, where ρ is the moon's density. For Phobos, Pandora and Epimetheus, such stresses are on the order of 10^5 dyne cm^{-2} (10^4 Pa) whereas the central hydrostatic pressures, $\sim\rho gr$, are about 10^6 dyne cm^{-2} (10^5 Pa) for these moons.

In real bodies, ones that have strength (represented by their elastic properties), these strains are less; this reduction can be substantial for small objects where the Love numbers are much below their ideal fluid values (Burns, 1986, p. 123), merely indicating that the "tidal" stresses are small fractions of their material strengths. Central density concentrations increase these distortions but not significantly (Murray and Dermott, 1999).

Over long times, many planetary ices will flow viscoelastically (when relatively warm) or plastically (for rubble piles); thus, by filling up the equipotential surface, they adopt the ideal shapes of fluid bodies. Hence ancient tidal stresses should have been accommodated by the present time. However, whenever the satellite orbits are slightly eccentric or inclined, tidal amplitudes are continually modulated over the orbital period. In the case of eccentric orbits, this occurs for two reasons: the planetary distance varies and also the satellite experiences an optical libration, meaning that a synchronously rotating satellite sees the planet's position in its sky rock back and forth, simply because it moves faster along its orbit at periapse and slower at apoapse (Murray and Dermott, 1999, Chs. 4 and 5; Tiscareno et al., 2009). As Wahr et al. (2009) point out, both of these effects produce stresses that are proportional to the orbital eccentricity e; an interested reader is referred to the latter paper to obtain the complex expressions of tidal stress but also because it provides a link to a web site where one can generate plots of stresses for any choice of relevant parameters. For our purposes, as seen in Table 1, the satellites of interest have small eccentricities (Phobos: 0.0151; Prometheus: 0.0022; Pandora: 0.0042; Epimetheus: 0.0098), and so the variable stresses due to the optical librations might be expected to only be $\sim 10^3$ dynes cm^{-2} (10^2 Pa).

However, this calculation of the planet's movement as seen from the satellite misses a possibly crucial aspect of the rotational motion of many small moons, including Epimetheus, and Phobos, and possibly Prometheus and Pandora. The elongated shapes of these bodies mean that their rotational librational frequencies are close to the orbit frequencies. As first noticed by Burns (1972) for the case of Phobos, this near-resonance induces forced rotational librations that are in phase with and enhance the optical librations that ultimately drive them. For Epimetheus, the measured physical libration of 5.9° (±1.2°) (Tiscareno et al., 2009) gives rise to tidal effects equivalent to those expected from an orbital eccentricity of an order of magnitude larger; Phobos's physical libration of ∼1° (Duxbury and Callahan, 1989; Simonelli et al., 1993; Willner et al., 2008) effectively doubles the effects of its eccentricity.

As given by Tiscareno et al. (2009), the angle between the moon's long axis and the direction to the planet, due to the combined optical and physical librations, is

$$\psi = \frac{2e \sin nt}{(\omega_0/n)^2 - 1},$$

where $(\omega_0/n)^2 = 3(B - A)/C$, and A, B, C are the moments of inertia about their respective axes. Under the assumption of a homogeneous ellipsoid,[1] the amplitude of this libration is roughly equal to $\psi_{\pi/2} = e\frac{a^2+b^2}{a^2-2b^2}$.

Using radii of (59.5, 43.5, 30.5) km and (51.5, 40, 32) km for Prometheus and Pandora, respectively, we thus expect significant augmentation in the libration of these satellites: 2.8° for Prometheus and 1.9° for Pandora. In both cases, the large majority of the amplitude is due to physical libration. While this result should be considered uncertain, since the interiors are likely to contain considerable void spaces and thus be non-homogeneous with inertial axes that may not be the geometric ones, our general conclusion from consideration of their shape is that significant forced librations of both Prometheus and Pandora are likely.

Two of the three close-in satellites on which we have reported organized swarms of grooves are those that also experience significant forced librations. Might Pandora be another with both grooves and forced librations? Because fewer high-resolution observations have been obtained by Cassini to date, Pandora has not yet been measured as similarly undergoing large forced librations, but it does have an elongated shape that makes it susceptible to such effects (as does Prometheus, which is so poorly imaged to date that neither grooves nor librations have been confirmed or ruled out). An alternate source of tidal effects on Pandora might be the chaotic variations in its orbit (French et al., 2003; Goldreich and Rappaport, 2003; Cooper and Murray, 2004; Renner et al., 2005) owing to kicks from an 118:121 resonance with Prometheus (Farmer and Goldreich, 2006), the F ring, and nearly resonant Mimas, which may occasionally cause short-term variations in tidal stressing.

It is uncertain whether stresses of 10^5–10^4 dyne cm^{-2} (10^4–10^3 Pa) are sufficient to produce noticeable geological features, such as grooves on these small moons. Soter and Harris (1977), in their discussion of failure on Phobos, list the material strengths of the lunar dusty regolith as low as we are demanding here. More recently, models of rubble piles, bodies with limited strengths, have become popular to account for the formation of binary asteroids (Merline et al., 2002), the distorted shapes of rubble-pile asteroids (Sharma, 2009), three of Saturn's ring-moons (Porco et al., 2007), and possibly the putative low strength of asteroids such as Eros (Asphaug, 2009). All of the saturnian satellites

[1] For an ellipsoid of constant internal density, $A \propto (b^2 + c^2)$ and $B \propto (a^2 + c^2)$ and $C \propto (a^2 + b^2)$.

discussed in this paper have very low densities (see Table 1), suggesting considerable pore space and likely low strength.

6. Conclusions

Grooves on Phobos and Epimetheus, both of which are known to be subject to tidal stress due to significant rotational librations, tend to occur as well-organized sets of parallel members. This correlation is prima facie evidence that variable tidal stresses induced by these oscillations are strong enough to fracture bodies. On both Phobos and Epimetheus, the planes that define some of these groove sets reflect the stress orientations due to tidal stresses in which the length of the groove is perpendicular to the tensile stress, as predicted by graben morphology.

Pandora has grooves similar to those on Phobos and Epimetheus, while current data can neither confirm nor rule out grooves on Prometheus. Both Prometheus and Pandora have a prolate shape and sufficient orbital eccentricity to make forced librations likely, though they have not been confirmed. We suggest that the grooves observed on Pandora, by analogy to Phobos and Epimetheus, may be further evidence of rotational libration.

Small bodies that do not match these conditions, such as fast-rotating or non-librating satellites, as well as asteroids, show groove patterns that are less well-organized on global scales. The latter may result from effects of multiple impact events.

Most grooves on all these objects remain best explained by regolith response to fractures in the underlying body. A few groove-like forms on small objects may be related to secondary ejecta, but these are the exceptions. The efficacy of tidal/rotational stresses in forming grooves suggests very weak materials make up many small bodies.

Acknowledgments

This research was supported by a NSF grant through the Research Experiences for Undergraduates (REU) Program as well as the Cassini Project under JPL contracts 13524799 and 13524800. M.S.T. acknowledges support from NASA's Cassini Data Analysis Program (NNX08AQ72G). J.A.B. acknowledges support from NASA's Planetary Geology and Geophysics Program (NNX08AL25G). We thank K. Consroe, B. Carcich, and P. Smith for technical assistance. In addition we thank our reviewers for their thoughtful comments and suggestions.

References

Aggarwal, H.R., Oberbeck, V.R., 1974. Roche limit of a solid body. Astrophys. J. 191, 577–588.
A'Hearn, M.F., and 32 colleagues, 2005. Deep impact: Excavating Comet Tempel 1. Science 310, 258–264.
Asphaug, E., 2009. Shattered dirt: Surface fracture of granular asteroids. Lunar Planet. Sci. 40 (abstract #1438).
Asphaug, E., Moore, J.M., Morrison, D., Benz, W., Nolan, M.C., Sullivan, R., 1996. Mechanical and geological effects of impact cratering on Ida. Icarus 120, 158–184.
Brownlee, D.E., and 11 colleagues, 2004. Surface of young Jupiter family Comet 81 P/Wild 2: View from the Stardust Spacecraft. Science 304, 1764–1769.
Buczkowski, D.L., Barnouin-Jha, O.S., Prockter, L.M., 2008. 433 Eros lineaments: Global mapping and analysis. Icarus 193, 39–52.
Burns, J.A., 1972. Dynamical characteristics of Phobos and Deimos. Rev. Geophys. Space Phys. 10, 463–483.
Burns, J.A., 1978. The dynamical evolution and origin of the martian moons. Vistas Astron. 22, 193–210.
Burns, J.A., 1986. The evolution of satellite orbits. In: Burns, J.A., Matthews, M.S. (Eds.), Satellites. University Arizona Press, Tucson, pp. 117–158.
Carr, M.H., Kirk, R.L., McEwen, A., Veverka, J., Thomas, P., Head, J.W., Murchie, S., 1994. The geology of Gaspra. Icarus 107, 61–71.
Cooper, N.J., Murray, C.D., 2004. Dynamical influences on the orbits of Prometheus and Pandora. Astron. J. 127, 1204–1217.
Croft, S.K., 1992. Proteus – Geology, shape, and catastrophic destruction. Icarus 99, 402–419.
Dombard, A.J., Freed, A.M., 2002. Thermally induced lineations on the Asteroid Eros: Evidence of orbit transfer. Geophys. Res. Lett. 29, 651–654.
Durda, D.D., 2009. Constraining source crater regions for boulder tracks and elongated secondary craters on Eros. Lunar Planet. Sci. 40 (abstract #2173).
Duxbury, T.C., Callahan, J.D., 1989. Phobos and Deimos control networks. Icarus 77, 275–286.
Farmer, A.J., Goldreich, P., 2006. Understanding the behavior of Prometheus and Pandora. Icarus 180, 403–411.
French, R.G., McGhee, C.A., Dones, L., Lissauer, J.J., 2003. Saturn's wayward shepherds: The peregrinations of Prometheus and Pandora. Icarus 162, 143–170.
Fujiwara, A., and 21 colleagues, 2006. The rubble-pile Asteroid Itokawa as observed by Hayabusa. Science 312, 1330–1334.
Gladman, B., 2007. Origin and evolution of Phobos and Deimos. LPI Contribution No. 1377, p. 18.
Goldreich, P., Rappaport, N., 2003. Origin of chaos in the Prometheus–Pandora system. Icarus 166, 320–327.
Head, J.W., Cintala, M.J., 1979. Grooves on Phobos: Evidence for possible secondary cratering origin. Reports of Planetary Geology Program 1978–1979, 19–21.
Horstman, K.C., Melosh, H.J., 1989. Drainage pits in cohesionless materials – Implications for the surface of Phobos. J. Geophys. Res. 94, 12433–12441.
Housen, K.R., Wilkening, L.L., 1982. Regoliths on small bodies in the Solar System. Annu. Rev. Earth Planet. Sci. 10, 355–376.
Jacobson, R.A., Spitale, J., Porco, C.C., Beurle, K., Cooper, N.J., Evans, M.W., Murray, C.D., 2008. Revised orbits of Saturn's small inner satellites. Astron. J. 135, 261–263.
Keller, H.U., Barbieri, C., Koschny, D., Lamy, P., Rickman, H., Rodrigo, R.OSIRIS Team, 2008. The Rosetta Asteroid Steins flyby observed by OSIRIS. Bull. Am. Astron. Soc. 40, 442.
Konopliv, A.S., Yoder, C.F., Standish, E.M., Yuan, D. -N., Sjogren, W.L., 2006. A global solution for the Mars static and seasonal gravity, Mars orientation, Phobos and Deimos masses, and Mars ephemeris. Icarus 182, 23–50.
Merline, W.J., Weidenschilling, S.J., Durda, D.D., Margot, J.L., Pravec, P., Stoores, A.D., 2002. Asteroids do have satellites. In: Bottke, W.F., Cellino, A., Paolicchi, P., Binzel, R.P. (Eds.), Asteroids III. University Arizona Press, pp. 289–312.
Morrison, S.J., Thomas, P.C., Veverka, J., Burns, J.A., Tiscareno, M.S., Porco, C.C., 2008. Grooves on small saturnian satellites: Possible evidence for tidal stressing. Bull. Am. Astron. Soc. 40, 479.
Murray, C.D., Dermott, S.F., 1999. Solar System Dynamics. Cambridge University Press, pp. 130-225.
Murray, J.B., Rothery, D.A., Thornhill, G.D., Muller, J.-P., Iliffe, J.C., Day, T., Cook, A.C., 1994. The origin of Phobos' grooves and crater chains. Planet. Space Sci. 42, 519–526.
Murray, J.B., Iliffe, J.C., Muller, J.-P., Neukum, G., Werner, S., Balme, M.HRSC Co-Investigator Team, 2006. New evidence on the origin of Phobos' parallel grooves from HRSC Mars Express. Lunar Planet. Sci. 37 (abstract #2195).
Neukum, G., Jaumann, R., Hoffmann, H., Behnke, T., Pischel, R., Roatsch, T., Hauber, G.A.E., Oberst, J., HRSC Co-Investigator Team, 2000. Imaging Goals and Capabilities of the HRSC camera experiment onboard Mars Express. Lunar Planet. Sci. 31 (abstract #1906).
Pappalardo, R.T., 2006. Ridge and trough terrains on outer planet satellites. AGU Fall Meeting (abstract #P32A-02A2).
Porco, C.C., and 19 colleagues, 2004. Cassini imaging science: Instrument characteristics and anticipated scientific investigations at Saturn. Space Sci. Rev. 115, 363–497.
Porco, C.C., and 34 colleagues, 2005. Cassini imaging science: Initial results on Phoebe and Iapetus. Science 307, 1237–1242.
Porco, C.C., Thomas, P.C., Weiss, J.W., Richardson, D.C., 2007. Saturn's small inner satellites: Clues to their origins. Science 318, 1602–1605.
Prockter, L., Thomas, P., Robinson, M., Joseph, J., Milne, A., Bussey, B., Veverka, J., Cheng, A., 2002. Surface expressions of structural features on Eros. Icarus 155, 75–93.
Renner, S., Sicardy, B., French, R.G., 2005. Prometheus and Pandora: Masses and orbital positions during Cassini's tour. Icarus 174, 230–240.
Richardson, J.E., Thomas, P.C., 2007. Modeling the cratering records of Hyperion and Phoebe: Indications of a shallow-sloped impactor population. Bull. Am. Astron. Soc. 39, 430.
Robinson, M.S., Thomas, P.C., Veverka, J., Murchie, S.L., Wilcox, B.B., 2002. The geology of 433 Eros. Meteorit. Planet. Sci. 37, 1651–1684.
Saito, J., and 33 colleagues, 2006. Detailed images of Asteroid 25143 Itokawa from Hayabusa. Science 312, 1341–1344.
Sharma, I., 2009. Equilibrium shapes of rubble-pile binaries: The Darwin ellipsoid for gravitationally held granular aggregates. Icarus 200, 636–654.
Simonelli, D.P., Thomas, P.C., Carcich, B.T., Veveraka, J., 1993. The generation and use of numerical shape models for irregular Solar System objects. Icarus 103, 49–61.
Soter, S., Harris, A., 1977. Are striations on Phobos evidence for tidal stress? Nature 268, 421–422.
Squyres, S.W., Croft, S.K., 1986. The tectonics of icy satellites. In: Burns, J.A., Matthew, M.S. (Eds.), Satellites. University Arizona Press, Tucson, pp. 293–341.
Sullivan, R., and 17 colleagues, 1996. Geology of 243 Ida. Icarus 120, 119–139.
Thomas, P.C., 1993. Gravity, tides, and topography on small satellites and asteroids – Application to surface features of the martian satellites. Icarus 105, 326–344.
Thomas, P.C., 1998. Ejecta emplacement on the martian satellites. Icarus 131, 78–106.
Thomas, P., Veverka, J., Bloom, A., Duxbury, T., 1979. Grooves on Phobos – Their distribution, morphology and possible origin. J. Geophys. Res. 84, 8457–8477.

Thomas, P.C., Veverka, J., Simonelli, D., Helfenstein, P., Carcich, B., Belton, M.J.S., Davies, M.E., Chapman, C., 1994. The shape of Gaspra. Icarus 107, 23–36.
Thomas, P.C., Belton, M.J.S., Carcich, B., Chapman, C.R., Davies, M.E., Sullivan, R., Veverka, J., 1996. The Shape of Ida. Icarus 120, 20–32.
Thomas, P.C., and 11 colleagues 1999. Mathilde: Size, shape, and geology. Icarus 140, 17–27.
Thomas, P.C., and 18 colleagues, 2002. Eros: Shape, topography, and slope processes. Icarus 155, 18–27.
Thomas, P.C., and 14 colleagues 2007. The shape, topography, and geology of Tempel 1 from deep impact observations. Icarus 187, 4–15.
Tiscareno, M.S., Burns, J.A., Thomas, P.C., 2009. The rotation of Janus and Epimetheus. Icarus, in press.
Van der Pluijim, B.A., Marshak, S., 2004. Earth Structure. W.W. Norton & Company, New York. pp. 114–137.
Veverka, J., Duxbury, T.C., 1977. Viking observations of Phobos and Deimos – Preliminary results. J. Geophys. Res. 82, 4213–4223.
Veverka, J., Thomas, P., Simonelli, D., Belton, M.J.S., Carr, M., Chapman, C., Davis, M.E., Greeley, R., Greenberg, R., Head, J., 1994. The discovery of grooves on Gaspra. Icarus 107, 72–83.
Veverka, J., and 16 colleagues, 1997. NEAR's Flyby of 253 Mathilde: Images of a C Asteroid. Science 278, 2109–2114.
Wahr, J., Selvans, Z.A., McCall, E.M., Barr, A.C., Collins, G.C., Selvans, M.M., Pappalardo, R.T., 2009. Modeling stresses on satellites due to non-synchronous rotation and orbital eccentricity using gravitational potential theory. Icarus 200, 188–206.
Weidenschilling, S.J., 1979. A possible origin for the grooves on Phobos. Nature 282, 697–698.
Willner, K., Oberst, J., Giese, B., Wahlisch, K.-D., Matz, T., Roatsch, T., Hoffmann, H., 2008. Studies of Phobos' orbit, rotation, and shape using spacecraft image data. In: ISPRS Congress Beijing, Proceedings of Commission IV, vol. XXXVII (B4), pp. 981–986. <http://www.isprs.org/congresses/beijing2008/proceedings/tc4.aspx>.
Wilson, L., Head, J., 2005. Dynamics of groove formation on Phobos by ejecta from Stickney Crater: Predictions and tests. Lunar Planet. Sci. 36 (abstract #1186).